

CATALYSIS BY METAL OXIDES

Catalytic Oxidation of Propylene. 11. An Investigation of the Kinetics and Mechanism over Iron-Antimony Oxide

George W. Keulks* and Man-Yin Lo

Department of Chemistry and Laboratory for Surface Studies, University of Wisconsin—Milwaukee, Milwaukee, Wisconsin 53201 (Received: February 26, 1986)

The kinetics of propylene oxidation over iron-antimony oxide (atomic ratio Sb/Fe = 4) were determined over the temperature range 325–475 °C, at 25 °C intervals by using a single-pass flow reactor. Propylene labeled selectively with D or ¹³C in a variety of positions and oxygen-18 were used as tracers to probe the mechanistic details of the reaction. Mass spectrometry and NMR were used to analyze the isotopic content of the acrolein produced. The rate of the reaction was dependent upon the partial pressures of both propylene and oxygen over the entire temperature range. The kinetics could be explained in terms of the coupled reaction of catalyst reduction and reoxidation. The kinetics suggested that the rate of catalyst reoxidation is slower than the rate of reduction and the oxidation of propylene takes place on a partially reduced catalyst surface. Deuterated propylene studies showed that the rate-determining step is the abstraction of an allyl hydrogen from propylene to form a π -allyl intermediate at all temperatures. Subsequent addition of oxygen to the π -allyl intermediate before the abstraction of a second hydrogen yields a σ -allyl species. This σ -allyl species is subsequently converted to the product acrolein. Oxygen-18 data showed that 1.6 and 2.6 layers of oxygen participate in the formation of both acrolein and carbon dioxide at 400 and 450 °C, respectively. This suggested that lattice oxygen is the selective oxygen for product formation. At lower temperatures (<350 °C), only 0.8 layer of oxygen participates in the formation of products. This suggested that adsorbed oxygen may become the possible source of selective oxygen for product formation at low temperatures. Both kinetics and tracer studies showed that carbon dioxide is formed exclusively through the further oxidation of acrolein.

Introduction

In addition to the well-known bismuth molybdate catalysts for the selective oxidation of propylene,^{1,2} binary oxides of antimony with metals such as iron,³ tin,⁴ and uranium⁵ have also been shown to be effective catalysts for the selective oxidation of propylene. Earlier studies on the properties of the iron-antimony system showed that the selectivity and activity of the catalyst is dependent on the antimony content of the catalyst.^{6,7} The selectivity of the catalyst increased dramatically when the Sb/Fe ratio was increased from 1 to 2 or greater.

The mechanism of propylene oxidation over bismuth molybdate catalysts has been extensively studied, and several comprehensive reviews have appeared in the literature.^{8,9} Studies concerning the kinetics and mechanism for the selective oxidation of propylene over iron-antimony oxide, however, are much more limited and the details of the mechanism have only recently begun to emerge.

Aso et al.¹⁰ studied the kinetics for the oxidation of propylene over iron-antimony oxide and the reduction of the catalyst with propylene. They suggested that the rate-determining step is the addition of a surface oxygen species to the π -allyl intermediate. Similar kinetic studies by Burrington et al.¹¹ on bismuth molybdate

and iron-antimony catalysts indicated that the rate-determining step is the abstraction of an allylic hydrogen to produce a π -allyl intermediate. Their results also suggested that the π -allyl intermediate is rapidly converted to a σ -allyl intermediate which subsequently is rapidly converted to acrolein.

Studies on related antimony-based catalysts, such as tin-antimony oxide and uranium antimonate suggest that antimony-based catalysts may differ mechanistically from bismuth molybdate catalysts. Portefaix et al.¹² studied the oxidation of deuterated propylene (CD₂=CHCH₃) over tin-antimony and Keulks et al.¹³ studied the oxidation of propylene-2,3,3,3-d₄ over uranium-antimony. Both studies showed that the initial step of the reaction is the same as the initial step over bismuth molybdate catalysts in which a symmetrical allylic intermediate is formed by the abstraction of an allylic hydrogen from propylene. However, the second hydrogen abstraction-oxygen addition sequence is different from the bismuth molybdate catalysts. With these antimony-based catalysts, the addition of oxygen to the allylic intermediate is suggested to take place prior to the second hydrogen abstraction.^{11,13}

Oxidation of propylene to acrolein takes place in an oxidizing atmosphere and the type of oxygen species, whether gaseous or lattice, used for product formation has been the topic of active research. Keulks¹⁴ used oxygen-18 as a probe to study the type of oxygen used for product formation for the oxidation of propylene over bismuth molybdate catalysts. Lattice oxygen was shown to be the direct source of oxygen for product formation. It is now well established that bismuth molybdate catalysts function through a Mars and van Krevelen mechanism.¹⁵ In this mechanism,

(1) Veatch, F.; Callahan, J. L.; Millberger, E. C.; Forman, R. W. *2nd Acetes Int. Congr. Catal. Paris 1960* **1961**, 2, 2647.

(2) Hearne, G. W.; Furman, K. W. U.S. Patent 2991 320, 1961.

(3) Callahan, J. L.; Gertisser, B. Belgian Patent 633 452, 1963.

(4) Bethall, T.; Hadley, D. T. U.S. Patent 3 094 565, 1963.

(5) Callahan, J. L.; Grasselli, R. K.; Gertisser, B. Belgian Patent 633 450, 1963.

(6) Boreskov, G. K.; Ven'yaminov, S. A.; Tarasova, D. V.; Dindoin, V. M.; Sazonova, N. N.; Olen'kova, I. P.; Kefeli, L. M. *Kinet. Katal.* **1969**, 10, 1530.

(7) Fattore, V.; Fuhrman, Z. A.; Manara, G.; Notari, B. *J. Catal.* **1975**, 37, 223.

(8) Keulks, G. W.; Krenzke, L. D.; Notermann, T. M. *Adv. Catal.* **1978**, 27, 183.

(9) Grasselli, R. K.; Burrington, J. D. *Adv. Catal.* **1981**, 30, 133.

(10) Aso, I.; Furukawa, S.; Yamazoe, N.; Seiyama, T. *J. Catal.* **1980**, 63, 29.

(11) Burrington, J. D.; Kartisek, C. T.; Grasselli, R. K. *J. Catal.* **1984**, 87, 363.

(12) Portefaix, J. L.; Figueras, F.; Forissier, M. *J. Catal.* **1980**, 63, 307.

(13) Keulks, G. W.; Yu, Z.; Krenzke, L. D. *J. Catal.* **1983**, 84, 38.

(14) Keulks, G. W. *J. Catal.* **1970**, 19, 232.

(15) Mars, P.; van Krevelen, D. W. *Chem. Eng. Sci. Suppl.* **1954**, 3, 41.

propylene is oxidized on active centers of the catalyst and lattice oxygen atoms are incorporated into the product acrolein. Gaseous oxygen serves to replenish the lattice oxygen removed from the catalyst.

Moro-oka et al.¹⁶ used oxygen-18 as a probe to study the oxidation of propylene over iron-antimony with varying antimony content at 450 °C using a circulating system. They found that only 4–7 layers of lattice oxygen participated in the formation of products depending upon the antimony content of the catalyst. In contrast, bismuth molybdate catalysts exhibit extensive participation of lattice oxygen in the formation of products.¹⁷

The present study employed a flow system in order to study the kinetics and mechanism of propylene oxidation over iron-antimony catalysts over a wide temperature range. Oxygen-18 and ¹³C- and ²H-labeled propylene were used as tracers to probe the mechanistic details of the reaction.

Experimental Section

Catalyst Preparation. The reagents used for catalyst preparation were Alfa Division of Ventron Corp. 99.7% antimony(III) oxide, Mallinckrodt AR-grade ferric nitrate and Hi-Pure electronic-grade ammonium hydroxide. Iron-Antimony catalysts with an Sb/Fe ratio (atomic) of 4 were prepared according to the following method.

Ferric nitrate [Fe(NO₃)₃·9H₂O] was heated to 60 °C until all the ferric nitrate was melted. The required amount of antimony(III) oxide was then added to the ferric nitrate solution and stirred. This mixture was heated to 80 °C in a water bath until brown fumes were no longer evolved. The resulting solution was neutralized with ammonium hydroxide, filtered, dried, and calcined in air at 500 °C for 20 h and 900 °C for 2 h. The resulting catalyst was used for the kinetics and mechanism studies without further activation.

Characterization of Catalyst. X-ray Powder Pattern. A GE XRD-5 diffractometer utilizing Cu K α radiation ($\lambda = 1.5418 \text{ \AA}$) was used for the X-ray diffraction pattern measurement.

Surface Area. The surface areas of the catalysts prepared for this study were determined by the BET method using N₂ as the adsorbate at liquid nitrogen temperature.

Apparatus. The reactor system used was a single-pass flow reactor and all experiments were conducted at atmospheric pressure. The general features of this system have been discussed earlier by Krenzke and Keulks.¹⁷

The feed gases, oxygen (Amerigas 99%), propylene (Amerigas 97%), and helium diluent (Amerigas 99.9%), were used without further purification. The individual gas flows were controlled by Tylan mass flow controllers, Model FC-260. Carbon tetrachloride and deuterated chloroform were obtained from Amend Drug and Chemical Co. and Aldrich Chemical Co., respectively. NMR tubes (10 mm) were obtained from Wilmad Glass Co. Inc.

The isotopic tracers used for the mechanism studies were oxygen-18 (99 atom % ¹⁸O) obtained from BOC Limited Prochem., London, England. Propylene-2,3,3,3-*d*₄, propylene-1,1,2-*d*₃, propylene-1,1-*d*₂, propylene-2-*d*₁, propylene-3,3,3-*d*₃, and propylene-1-¹³C-3,3,3-*d*₃ (98 atom % D and 98 atom % ¹³C) were obtained from Merck, Sharp and Dohme Canada Ltd., Montreal, Canada. These labeled compounds were introduced into the feed stream by a variable speed syringe pump (Sage Instruments, Model 341) equipped with a 10-cm³ Hamilton gas-tight syringe.

The feed gas composition and product distribution were analyzed by a Packard Model 417 Becker gas chromatograph equipped with dual columns and an optional linear temperature programmer. Two stainless steel columns 1/4 in. × 6 ft, were packed with 80–100 mesh Poropak N. The composition of the feed and product gas streams were determined from the peak areas utilizing a Spectra-Physics Autolab System I computing integrator. The quantity of each component was calculated with peak areas and preprogrammed response factors.

TABLE I: Catalyst Charge-Temperature Relationship for Oxygen-18 Studies

temp, °C	wt of catalysts used, g	$\mu\text{g-atom of O}^{2-}$
450	0.60	8 537
400	0.90	12 827
350	1.16	16 449

An Uthe Technology International (UTI), Model 100C quadrupole mass analyzer was used to analyze the isotopic distribution of reaction products during the tracer experiments. The mass analyzer was coupled to the reactor-GC system by a Granville-Phillips variable leak valve. The output of the mass analyzer was interfaced to an IBM PC computer utilizing a UTI Model 100 SpectraLink interface. This allows the measurement of the maximum peak heights for all *m/e* values over the entire scan range.

A Bruker WM-250 NMR spectrometer operating in the pulsed Fourier transform mode was used to study the relative isotopic distribution of unreacted propylene and acrolein from the reaction.

Experimental Approach. Kinetic Data. Iron-antimony oxide with atomic ratio Sb/Fe = 4 was used for the kinetics and mechanism studies. The procedures used for determining the reaction orders and apparent activation energies have been reported earlier.^{17,32}

Mass Spectrometry Study. The feed gas composition and procedures for catalyst line-out and tracer addition were the same as reported previously.^{17,32} The catalyst charge-temperature relationship is given in Table I.

During the oxygen-18 experiments, the oxygen-18 concentrations in the gas-phase oxygen, carbon dioxide and acrolein were determined by repeatedly scanning the *m/e* range 25–65 with a scan time of 10–15 s at a pressure of 1×10^{-5} Torr. A minimum of 20 scans were recorded during each tracer experiment.

In the deuterated propylene experiments, the rate constants and the primary kinetic isotope effects for acrolein and carbon dioxide formation for the oxidation of CD₂=CDCH₃ and CH₂=CDCD₃ were determined from GC/MS measurements. The deuterium content of acrolein was determined from the ratio of CD₂=CD-CHO (*m/e* = 59) to CH₂=CDCDO (*m/e* = 58) by repeatedly scanning the mass range 54–62.

NMR Study. In the preparation of NMR samples, the reaction conditions were the same as the ones used for mass spectrometry studies. However, instead of direct introduction of the reactor effluent into the mass spectrometer, the reactor effluent was condensed in a trap maintained at 77 K. The material trapped at 77 K was then quickly transferred into an on-line preparative gas-chromatograph by replacing the cold trap with boiling water. Unreacted propylene and acrolein, separated by gas chromatography, were separately collected with a liquid N₂ trap. The samples were then vacuum transferred into two separate 10-mm NMR tubes containing carbon tetrachloride that was degassed with repeated freeze-pump-thaw cycles. The NMR tubes were sealed under vacuum. No internal lock was used since the same sample was used for the acquisition of ¹H, ²H, and ¹³C spectra. Samples for fresh, unreacted recovered, and products of the following propylenes were obtained: propylene-1,1-*d*₂, propylene-2-*d*₁, propylene-3,3,3-*d*₃, and propylene-1-¹³C-3,3,3-*d*₃. All spectra were measured at 297 K.

¹H spectra were obtained at 250 MHz. ²H spectra were obtained at 38.5 MHz and proton broad band decoupling was used. The individual deuterium signals were integrated and then measured by a ruler to determine the relative ratio of the different forms of recovered propylene (CD₂=CHCH₃ and CH₂=CHCD₃) and acrolein produced (CD₂=CHCHO, CH₂=CHCHO and CH₂=CHCDO) for each experiment. A typical number of transients for ²H spectra acquisition was 200. The chemical shift for ²H signals were determined with CDCl₃ as a reference. ¹³C spectra were obtained at 62.9 MHz and proton broad band decoupling was also used. The distribution of the different forms of ¹³C-labeled propylene and acrolein were determined both by weighing the peaks and by measuring the integrated signals by

(16) Moro-oka, Y.; Ueda, W.; Tanaka, S. *Proc. Int. Congr. Catal.*, 7th, 1981, B30.

(17) Krenzke, L. D.; Keulks, G. W. *J. Catal.* 1980, 64, 295.

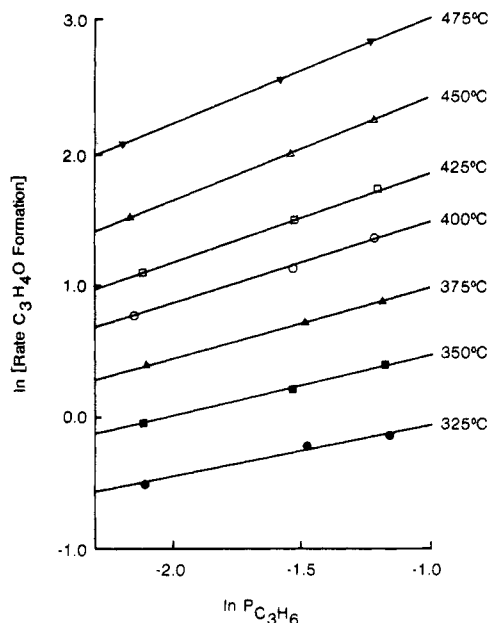


Figure 1. Propylene dependency for acrolein formation.

TABLE II: Reaction Orders for Propylene Oxidation

temp, °C	acrolein formation		carbon dioxide formation	
	C ₃ H ₆	O ₂	C ₃ H ₆	O ₂
475	0.8	0.3	0.7	0.8
450	0.8	0.3	0.7	0.7
425	0.7	0.3	0.6	0.7
400	0.6	0.3	0.6	0.7
375	0.5	0.3	0.5	0.7
350	0.5	0.4	0.4	0.6
325	0.4	0.4	0.3	0.4

a ruler. A typical number of transients was 500. Chemical shifts for ¹³C signals were determined relative to the solvent, e.g., 95.3 ppm for CCl₄.

Results

Characterization of Catalyst. The X-ray powder pattern for the catalyst prepared for the kinetic and mechanism studies indicated that the catalyst consists of two phases, α-Sb₂O₄¹⁸ and FeSbO₄.¹⁹ This is in good agreement with earlier reports.^{6,20-23}

The surface area of the catalyst as determined by the BET method was 5.25 m²/g. This value was used to calculate the specific activities and specific rate constants for the oxidation of propylene.

Kinetic Data. The reaction orders of propylene and oxygen in the formation of acrolein and carbon dioxide were determined from the following rate equation between 325 and 475 °C:

$$\text{rate} = k[\text{C}_3\text{H}_6]^m[\text{O}_2]^n \quad (1)$$

where k is the rate constant and m and n are the reaction orders for propylene and oxygen, respectively. A plot of $\ln(\text{rate})$ vs. $\ln(\text{partial pressure or the reactant being varied})$ will yield a straight line with slope equal to the reaction order of the reactant being

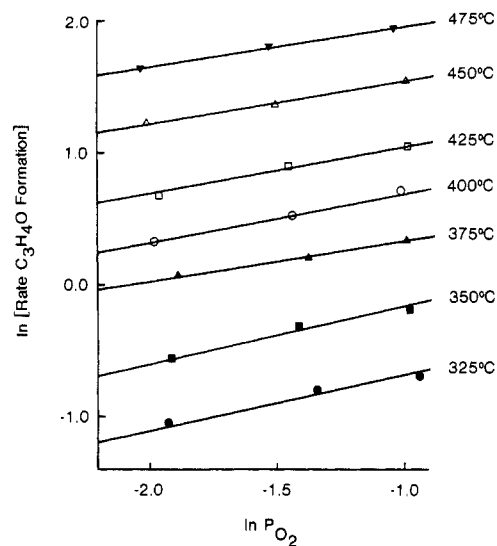


Figure 2. Oxygen dependency for acrolein formation.

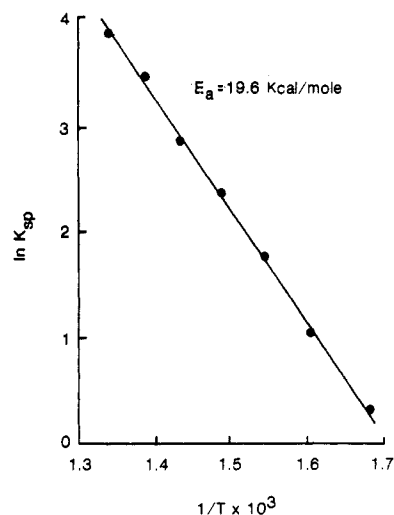


Figure 3. Arrhenius plot for acrolein formation.

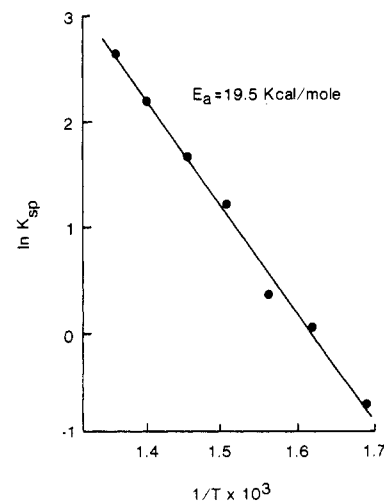


Figure 4. Arrhenius plot for CO₂ formation.

varied and a y intercept equal to $\ln k'$, where k' is a proportionally constant equal to $k[\text{reactant held constant}]^{m \text{ or } n}$. The plots for the dependence of propylene and oxygen for the formation of acrolein are shown in Figures 1 and 2, respectively. The reaction orders are summarized in Table II.

The specific rate constants for the formation of acrolein and carbon dioxide at a given temperature were calculated from the observed specific rate of formation and the reaction orders obtained

(18) *Inorganic Index to the Powder Diffraction Files*; American Society for Testing and Materials: Philadelphia, 1967.

(19) Brandt, K. *Ark. Chem., Mineral. Mag.* **1943**, *30*, 107.

(20) Fattore, V.; Furhrman, Z. A.; Manara, G.; Notari, B. *J. Catal.* **1975**, *37*, 223.

(21) Adamiya, T. V.; Mischchenko, Y. A.; Dulin, D. A.; Gel'bstein, A. I. *Kinet. Katal.* **1970**, *11*, 1160.

(22) Carbuicchio, M.; Centi, G.; Trifiro, F. *J. Catal.* **1985**, *91*, 85.

(23) Burriesci, N.; Garbassi, F.; Pettrera, M.; Petrini, G. *J. Chem. Soc., Faraday Trans. 1* **1982**, 817.

(24) Melander, L. *Isotope Effect on Reaction Rate*; Ronald Press: New York, 1960; p 22.

TABLE III: Oxidation of Propylene-1,1,2-d₃ and Propylene-2,3,3,3-d₄: k_H/k_D at 350, 400, and 450 °C

temp, °C	oxidation of propylene-1,1,2-d ₃		oxidation of propylene-2,3,3,3-d ₄ ^a	
	C ₃ H ₄ O	CO ₂	C ₃ H ₄ O	CO ₂
450	1.05 (1.0)	1.08 (1.0)	1.80 (1.8)	1.82 (1.8)
400	1.10 (1.0)	1.05 (1.0)	2.21 (2.0)	1.82 (2.0)
350	1.11 (1.0)	1.20 (1.0)	2.25 (2.2)	1.90 (2.2)

^aThe values in parentheses are the theoretical kinetic isotope effect calculated from infrared data and quantum mechanical according to Melander.²⁴

TABLE IV: Oxidation of Propylene-1,1,2-d₃ and Propylene-2,3,3,3-d₄ over Iron-Antimony Catalyst (Sb/Fe = 4): Ratio of the Two Forms of Deuterated Acrolein Obtained from Mass Spectrometric Studies

temp, °C	distn obsd for oxidation of propylene-1,1,2-d ₃		distn obsd for oxidation of propylene-2,3,3,3-d ₄	
	%	%	%	%
	CD ₂ =CDCHO	CH ₂ =CDCDO	CD ₂ =CDCHO	CH ₂ =CDCDO
450	46	54	51	49
400	50	50	50	50
350	77 ^a	23 ^a	48	52

^aObtained from the oxidation of CD₂=CHCH₃.

from the kinetic studies using eq 1. These specific rate constants were then used to calculate the apparent energies of activation for the formation of acrolein and carbon dioxide by using the Arrhenius equation. The Arrhenius plots for the formation of acrolein and carbon dioxide are shown in Figures 3 and 4, respectively.

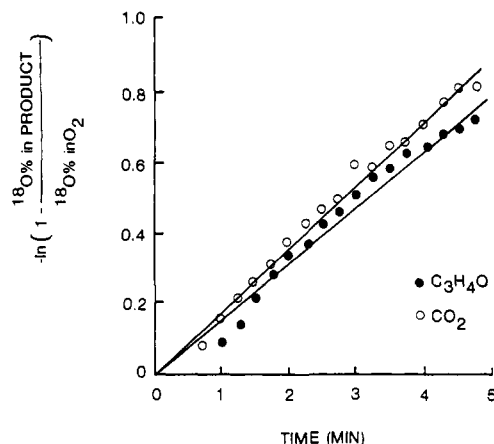
Mass Spectrometry Studies. Oxidation of Propylene-2,3,3,3-d₄ and Propylene-1,1,2-d₃. The conversion of propylene to acrolein requires the removal of two hydrogens (breaking of two C-H bonds) and an addition of an oxygen atom. If the rate-determining step involves the breaking of a C-H bond, a primary kinetic isotope effect will be observed if the hydrogen in the C-H bond is replaced by deuterium. In this study, two deuterated propylenes were used—propylene-1,1,2-d₃ and propylene-2,3,3,3-d₄. The rate constants for the oxidation of these deuterated propylenes, k_D , are compared with those obtained for unlabeled propylene, k_H . The experimental and theoretical k_H/k_D ratios for the formation of acrolein and carbon dioxide are given in Table III.

Two forms of deuterated acrolein (CD₂=CDCHO and CH₂=CDCDO) are expected to form from the oxidation of either of the deuterated propylenes if the reaction proceeds through a π -allylic intermediate. The isotopic distribution of deuterium in acrolein can be used to determine the second hydrogen abstraction-oxygen addition sequence for the formation of acrolein. Table IV shows the experimental deuterium distribution for the formation of acrolein.

Oxygen-18 Data. The purpose of using gas-phase oxygen-18 as a probe in this study is to determine whether adsorbed or lattice oxygen is the source of oxygen species for the formation of acrolein and carbon dioxide. The model used to determine the extent of lattice oxygen participation assumes that the reactive oxygen reservoir acts as an exponential dilution volume.¹⁷ The amount of oxygen participating in the formation of products can be calculated from the following equation:

$$\frac{\% \text{ }^{18}\text{O in product}}{\% \text{ }^{18}\text{O in O}_2} = 1 - e^{-Ft/V} \quad (2)$$

where F is the total flow of oxygen through the catalyst, which equals the rate of oxygen flow out of the catalyst as oxygenated products in $\mu\text{g-atom}/\text{min}$, t is the time for the addition of oxygen-18 in minutes, V is the amount of catalyst oxygen participating in the formation of a given product in $\mu\text{g-atoms}$, and ($\% \text{ }^{18}\text{O}$ in

**Figure 5.** ¹⁸O incorporation into acrolein and CO₂ over iron-antimony oxide (Sb/Fe = 4) at 450 °C.**TABLE V: Oxygen-18 Data**

temp, °C	% cat. O participation in formation of		no. O ^a layer participation in formation of	
	C ₃ H ₄ O	CO ₂	C ₃ H ₄ O	CO ₂
450	1.6	1.5	2.4	2.2
400	1.0	0.8	1.6	1.6
350	0.5	0.3	0.8	0.7

^aAssuming an oxygen packing of 1×10^{15} atoms/cm² and a catalyst composition of FeSbO₄ + $\frac{3}{2}\alpha\text{-Sb}_2\text{O}_4$ (Sb/Fe = 4).

product)/($\% \text{ }^{18}\text{O}$ in O₂) at time t can be determined by analyzing the oxygen-18 content in the reaction effluent by using the mass spectrometer. A plot of $-\ln [1 - ((\% \text{ }^{18}\text{O}$ in product)/($\% \text{ }^{18}\text{O}$ in O₂))] vs. the time t yields a straight line with a slope of F/V . The plot shown in Figure 5 for the reaction conducted at 450 °C is characteristic of all of the ¹⁸O experiments. The amount of catalyst oxygen and the number of oxygen layers participating in the formation of products were calculated from eq 2. The results are summarized in Table V.

NMR Measurements. Much of the mechanistic information concerning the sequence of steps from reactant to product has been gained from mass spectrometric analysis of the product acrolein. While this technique has proven to be extremely useful, it has limitations due to low sensitivity and the difficulty of analyzing the unreacted propylene for isomerization. The use of NMR spectroscopy with deuterated and ¹³C-labeled propylene offers distinct advantages.

Three labeled propylenes were used for the NMR study—¹³CH₂=CHCD₃, CD₂=CHCH₃, and CH₂=CHCD₃. For each, ¹H and ²H NMR spectra were obtained. For the ¹³C-labeled propylene, ¹³C NMR spectra were also obtained. Integration of the signals provided quantitative information concerning the location of the isotopic label.

Figure 6 shows the characteristic ¹H broad band decoupled ¹³C spectra for (a) the fresh propylene (¹³CH₂=CHCD₃), (b) the unreacted (recovered from the reaction) propylene, and (c) the acrolein formed from the oxidation of ¹³CH₂=CHCD₃ over the iron-antimony oxide catalyst.

Figure 7 shows the characteristic ¹H NMR spectrum of acrolein formed from the oxidation of either CD₂=CHCH₃ or CH₂=C-HCD₃. The same ¹H spectrum was obtained in either case and two signals were observed. One is assigned to the proton bonded to the carbonyl carbon (δ 9.5) and the other is assigned to the protons bonded to the methylene and methine carbons (δ 6.05–6.30). This ¹H NMR spectrum is identical with the literature reports for undeuterated acrolein.²⁵

(25) Sadler NMR Spectra; Sadler Research Laboratories: Philadelphia, 1967; 9153M.

(26) Halliday, J. D.; Bindner, P. E. *Can. J. Chem.* 1976, 54, 3775.

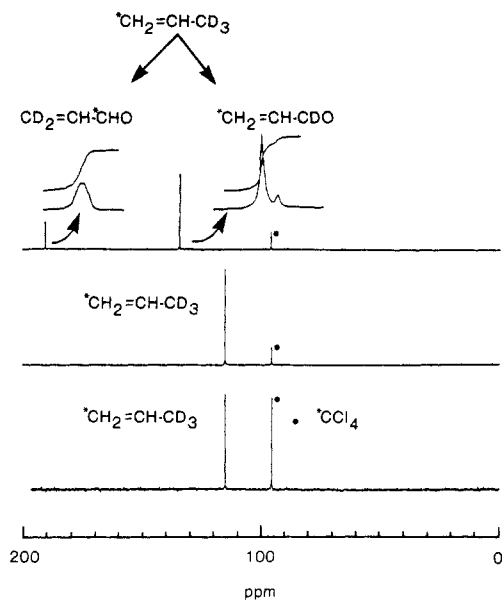


Figure 6. ^1H broad band decoupled ^{13}C NMR spectra of (a) fresh $^{13}\text{CH}_2=\text{CHCD}_3$, (b) unreacted $^{13}\text{CH}_2=\text{CHCD}_3$, and (c) acrolein formed by oxidizing $^{13}\text{CH}_2=\text{CHCD}_3$.

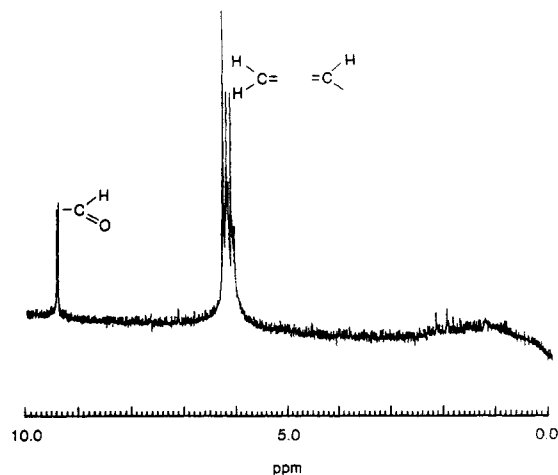


Figure 7. ^1H NMR spectrum of $\text{CH}_2=\text{CHCDO}$ and $\text{CD}_2=\text{CHCHO}$ formed by oxidizing $\text{CD}_2=\text{CHCH}_3$.

TABLE VI: Vicinal ^{13}C , D Coupling Constants for Acrolein

	calcd, ^a Hz	this study, Hz
$^3J(\text{CD})^t$	2.5	2.4
$^3J(\text{CD})^c$	1.6	1.6

^a Calculated from $^3J_{\text{CH}}/6.51$, $\gamma_{\text{H}}/\gamma_{\text{D}} = 6.51$.

TABLE VII: Relative Ratio of the Various Forms of Deuterated Propylene Recovered and Acrolein Formed with ^2H and ^{13}C NMR

reactant	temp, °C	acrolein		propylene	
		$-\text{CDO}^a$	CD_2^b	CD_2^b	$-\text{CD}_3$
$\text{CD}_2=\text{CHCH}_3$	450	50	50	93	7
	350	47	53	92	8
	325	50	50	96	4
$\text{CH}_2=\text{CHCD}_3$	450	48	52	<1	99+
	350	48	52	<1	99+
	325	49	51	<1	99+
$^{13}\text{CH}_2=\text{CHCD}_3$	450	49 ^c	51 ^d	2	98
	350	53	47	<1	99+
	325	53	47	<1	99+

^a $\text{CH}_2=\text{CHCDO}$. ^b $\text{CD}_2=\text{CHCHO}$. ^c $^{13}\text{CH}_2=\text{CHCDO}$. ^d $\text{CD}_2=\text{CH}^{13}\text{CHO}$.

Figure 8 shows the characteristic ^1H proton broad band decoupled ^2H NMR spectra for (a) the fresh $\text{CD}_2=\text{CHCH}_3$, (b) the recovered $\text{CD}_2=\text{CHCH}_3$, and (c) the acrolein formed from

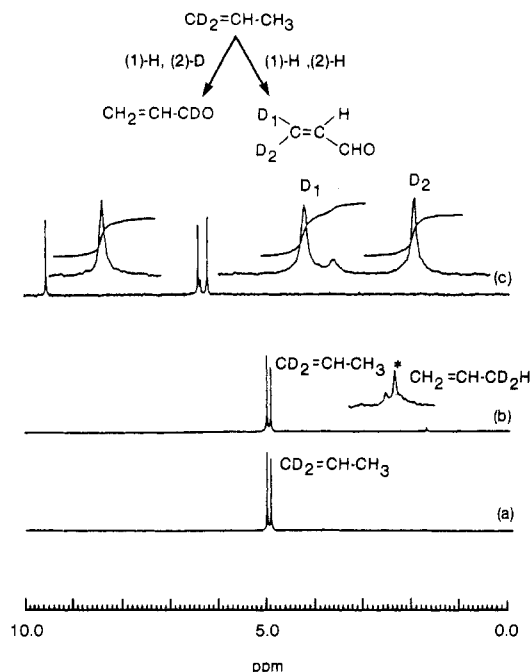


Figure 8. ^1H broad band decoupled ^2H NMR spectra of (a) fresh $\text{CD}_2=\text{CHCH}_3$, (b) unreacted $\text{CD}_2=\text{CHCH}_3$, and (c) acrolein formed by oxidizing $\text{CD}_2=\text{CHCH}_3$. Trace amounts (marked by an asterisk) of $\text{CH}_2=\text{CHCD}_2\text{H}$, $\text{CH}_2=\text{CHCD}_2\text{H}$, and $\text{CH}_2=\text{CHCD}_3$ were detected (see ref 26).

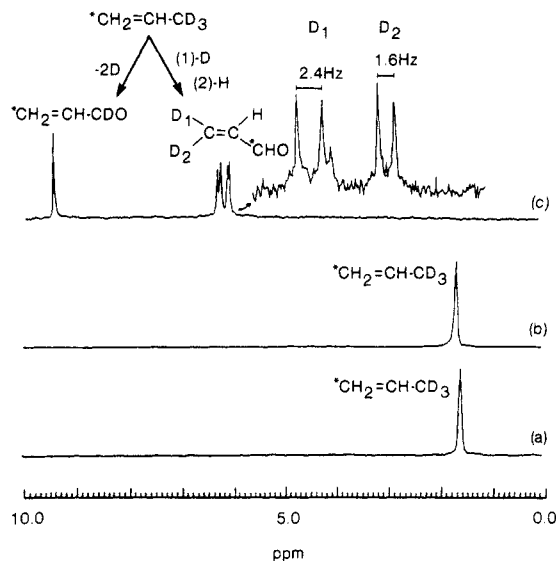


Figure 9. ^1H broad band decoupled ^2H NMR spectra of (a) fresh $^{13}\text{CH}_2=\text{CHCD}_3$, (b) unreacted $^{13}\text{CH}_2=\text{CHCD}_3$, and (c) acrolein formed by oxidizing $^{13}\text{CH}_2=\text{CHCD}_3$.

the oxidation of $\text{CD}_2=\text{CHCH}_3$ over iron-antimony. Figure 9 shows the same spectra for the oxidation of $^{13}\text{CH}_2=\text{CHCD}_3$.

Figure 10 shows the proton broad band decoupled ^2H NMR spectrum for the products formed from the oxidation of $\text{CD}_2=\text{CHCH}_3$. A trace amount of CDCl_3 (δ 7.24) was added as a reference.

Figure 11 shows the ^2H NMR spectrum for acrolein formed from the oxidation of $\text{CH}_2=\text{CDCH}_3$ over iron-antimony catalyst. Again, a trace amount of CDCl_3 was added as a reference.

Figure 12 shows the DEPT (distortionless enhancement by polarization transfer) ^{13}C spectrum of deuterated acrolein formed from the oxidation of $^{13}\text{CH}_2=\text{CHCD}_3$ over iron-antimony. No ^{13}C bonded to D was detected; only ^{13}C bonded to H was detected.

The ^2H and ^{13}C spectra were used to determine the ratio of the forms of deuterated (^{13}C -substituted) acrolein formed in the selective oxidation reaction. The ^2H and ^{13}C spectra for recovered propylene was used to determine the extent of isomerization of

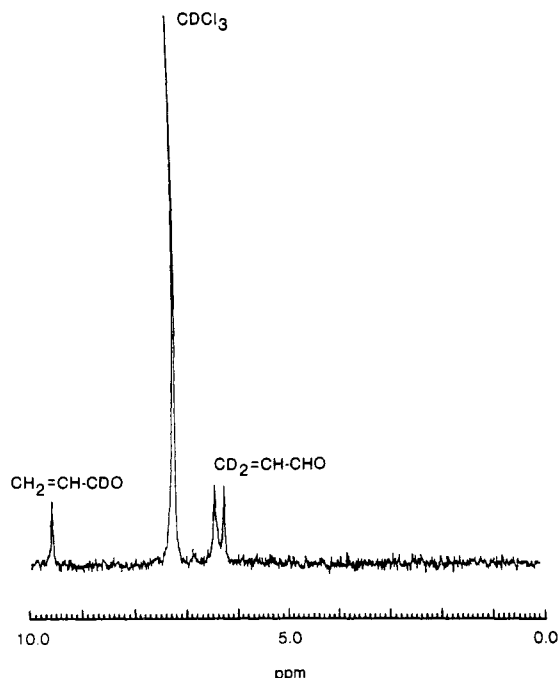


Figure 10. ^1H broad band decoupled ^2H NMR spectrum of acrolein produced during the oxidation of $\text{CH}_2=\text{CHCD}_3$, with CDCl_3 as a reference (δ 7.24).

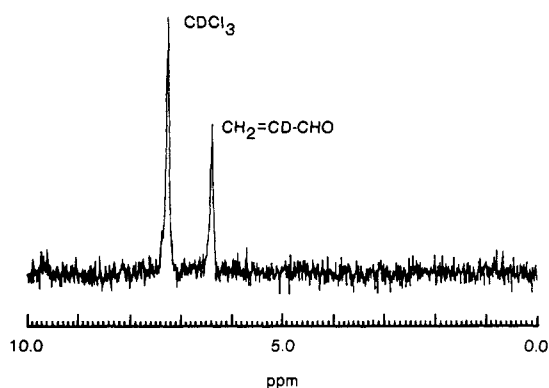


Figure 11. ^1H broad band decoupled ^2H NMR spectrum of acrolein produced during the oxidation of $\text{CH}_2=\text{CDCH}_3$, with CDCl_3 as a reference (δ 7.24).

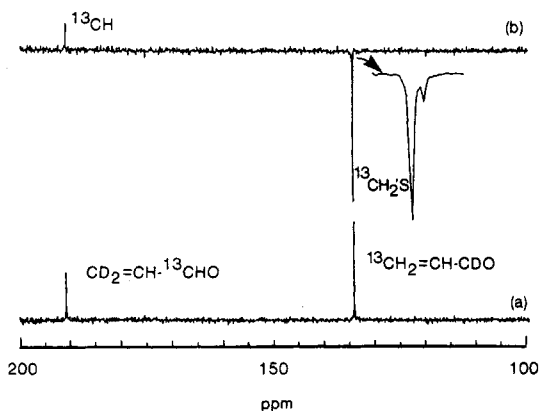


Figure 12. (a) ^{13}C broad band decoupled ^{13}C NMR spectrum of acrolein from $^{13}\text{CH}=\text{CHCD}_3$. (b) DEPT (distortionless enhancement by polarization transfer) ^{13}C spectrum of deuterated acrolein from $^{13}\text{CH}_2=\text{CHCD}_3$ (^{13}CH shown as a positive signal; $^{13}\text{CH}_2$ shown as a negative signal).

propylene during the reaction. The results are summarized in Table VII.

Vicinal carbon–deuterium couplings were observed for $\text{CD}_2=\text{CH}^{13}\text{CHO}$. The coupling constants are different for the coupling

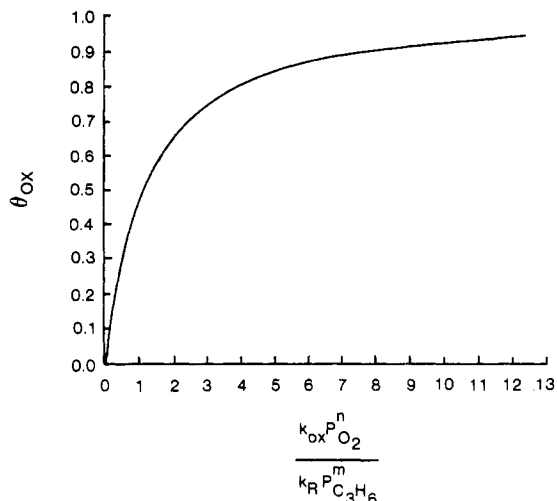
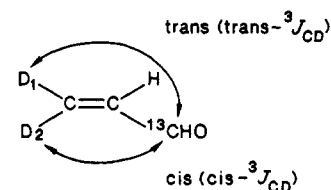


Figure 13. Fraction of fully oxidized sites vs. the ratio of the rate of reoxidation to the rate of reduction.

between the cis deuterium and the carbonyl carbon and the coupling between the trans deuterium and the carbonyl carbon.



The calculated²⁷ and experimentally determined coupling constants are summarized in Table VI.

Discussion

Characterization of Catalyst. A compound was formed between ferric oxide and antimony(III) oxide. The X-ray powder pattern showed that the compound formed has a composition of FeSbO_4 . The existence of two phases (FeSbO_4 and $\alpha\text{-Sb}_2\text{O}_3$) in the active catalyst is in good agreement with earlier studies by using XRD,^{6,21} IR,²⁸ and Mössbauer^{22,23} methods.

Kinetic Data. A redox mechanism is involved in the oxidation of propylene over iron–antimony oxide, especially at temperatures higher than 400 °C. The basic concept of this redox mechanism is that the lattice oxygen of a reducible metal oxide can serve as a useful oxidizing agent for hydrocarbons. Actually the formation of products and catalyst reduction proceed simultaneously.^{29–31} In order to maintain a continuous catalytic reaction, the catalyst oxygen must be continually replenished via reoxidation by the gas-phase oxygen. Details of this mechanism have been discussed elsewhere.^{17,32} Under steady-state conditions, the flow of oxygen into the catalyst equals the flow of oxygen out of the catalyst as oxygenated products. Therefore, the rate of catalyst reduction will equal to the rate of catalyst reoxidation, such that

$$\frac{\theta_{\text{OX}}}{1 - \theta_{\text{OX}}} = \frac{k_{\text{OX}} P^n_{\text{O}_2}}{k_{\text{R}} P^m_{\text{C}_3\text{H}_6}}$$

The relationship between the fraction of sites that is oxidized (θ_{OX}) and the ratio of the rate of reoxidation to the rate of reduction is shown graphically in Figure 13.

In cases where the rate of reoxidation is much greater than the rate of reduction (the right-hand portion of Figure 13), the number

(27) Vogeli, U.; von Philipsborn, W. *Org. Magn. Reson.* **1975**, *7*, 617.

(28) Sala, F.; Trifiro, F. *J. Catal.* **1976**, *41*, 1.

(29) Yamazoe, N.; Aso, I.; Amamoto, T.; Seiyama, T. *Proc. Int. Congr. Catal.*, **7th 1981**, B41.

(30) Aykan, K. *J. Catal.* **1968**, *12*, 281.

(31) Batist, Ph. A.; Prette, H. J.; Schuit, G. C. A. *J. Catal.* **1969**, *15*, 267.

(32) Monnier, J. R.; Keulks, G. W. *J. Catal.* **1981**, *68*, 51.

of oxidized sites, θ_{OX} , remains constant. This suggests that the overall rate of propylene oxidation is controlled primarily by the rate of reduction according to the following equations:

$$\text{rate} = k_R P_{C_3H_6}^m \theta_{OX} = k' R_{C_3H_6}^m$$

where, $k' = k_R \theta_{OX}$.

Keulks et al.^{17,32} showed that the oxidation of propylene over bismuth molybdate catalysts follows this rate equation with $m = 1$ at temperatures over 400 °C.

In cases where the rate of reduction is much greater than the rate of reoxidation, the reaction rate tends to be reoxidation limited and is represented as follows:

$$\text{rate} = k_{OX} P_{O_2}^n (1 - \theta_{OX}) = k_{OX} P_{O_2}^n \theta_{OX}$$

where $\theta_{OX} \ll 1$.

In the oxidation of propylene over cuprous oxide, Isaev et al.³³ found that the rate of reaction follows this equation with $n = 1$, and the reaction is independent on the partial pressure of propylene.

However, in the transition from the reduction-limited region to the reoxidation-limited region, the observed kinetics would be a composite of both the reoxidation and reduction kinetics with medium coverage and partial dependencies in both propylene and oxygen will be observed. This kinetic relationship has been observed for the oxidation of propylene over bismuth molybdate catalysts at temperatures <400 °C and over tin-antimony oxide.

In the present study, partial reaction orders in both reactants are observed at all temperatures, indicating that the overall kinetics are a composite of the reoxidation and reduction kinetics. The calculated θ_{OX} is between 0.5 and 0.7 monolayer. This suggests that the oxidation of propylene takes place over a partially reduced surface. The rate of reoxidation is much slower than the rate of reoxidation observed for bismuth molybdates.

Similar results have been reported for the oxidative dehydrogenation of *n*-butene³⁴ and for the oxidation of propylene over tin-antimony catalysts.³⁵ In both studies, the rate of reaction is dependent on the partial pressure of both propylene and oxygen. Furthermore, in the oxidative dehydrogenation of *n*-butene over iron-antimony oxide, partial orders in both *n*-butene and oxygen were observed.³⁶ These similarities in kinetics and mechanism for these antimony-based catalysts suggest that the catalytic properties of these catalysts are very similar and antimony plays a major role in the oxidation reaction.

The apparent energies of activation for the formation of acrolein and carbon dioxide are the same, equal to 19.5–19.6 kcal/mol. These values are consistent with the theoretical value recently reported for the activation of propylene.³⁷ This also suggests that acrolein and carbon dioxide are produced from the same intermediate.

Carbon dioxide can be formed by a parallel reaction (direct oxidation of propylene) or by a consecutive reaction (further oxidation of acrolein). The same reaction orders on propylene partial pressure, the same apparent activation energies, and the same kinetic isotope effects suggest that a common intermediate is responsible for the formation of both acrolein and carbon dioxide and, together with the oxygen-18 data, suggest that carbon dioxide is formed exclusively by the consecutive oxidation of acrolein.

Mechanistic Details Obtained by Mass Spectrometry. The oxygen-18 data in Table V indicate that only a few layers of lattice oxygen participate in the formation of both acrolein and carbon dioxide. This is quite different from the bismuth molybdate catalysts in which multilayers of lattice oxygen are involved in the formation of products but quite similar to the results obtained with U-Sb catalysts.¹³ At 400 and 450 °C, 1.6 and 2.6 layers

of oxygen participate in both the formation of acrolein and carbon dioxide. This suggests that iron-antimony catalysts also function via a redox mechanism in which lattice oxygen is the direct source of oxygen for product formation. However, at 350 °C, less than one monolayer of oxygen participates in the formation of products, suggesting that adsorbed oxygen may be the oxygen species for the formation of products. These results are in good agreement with those reported by Yamazoe et al.,²⁹ Moro-oka et al.,¹⁶ and Burrington et al.¹¹ using other methods. They, too, showed that only a few layers of lattice oxygen are used for the formation of products. Within experimental error, the amount of oxygen participating in the formation of carbon dioxide is equal to the amount participating in the formation of acrolein. Therefore, there appears to be no distinction between the oxygen incorporated into the carbon dioxide and acrolein. This suggests that carbon dioxide is formed by the further oxidation of acrolein.

In the studies utilizing deuterated propylene, a primary kinetic isotope effect is observed for the oxidation of $CH_2=CD_2$ at all temperatures. However, no primary kinetic isotope effect is observed for the oxidation of $CD_2=CD_2$. These results suggest that the rate-determining step is the abstraction of a hydrogen from the allylic carbon. The distribution of deuterium in the products indicate that equal amounts of $CD_2=CDCHO$ and $CH_2=CDCHO$ are formed no matter which propylene is used as the starting material. This suggests that both deuterated propylenes give rise to a common intermediate, most likely a symmetrical π -allyl species. Furthermore, the formation of equal amounts of $CD_2=CDCHO$ and $CH_2=CDCHO$ indicate that the addition of oxygen most likely takes place prior to the abstraction of a second hydrogen. This observation is consistent with the results reported by Keulks et al.¹³ for uranium antimonate catalysts, by Portefaix et al.¹¹ for tin-antimony catalysts, and by Burrington et al.¹¹ for iron-antimony catalysts.

Mechanistic Details Obtained by NMR. The use of NMR spectroscopy provides additional details concerning the structure of the acrolein formed as well as information concerning the extent of double bond isomerization in the unreacted propylene. This additional information is valuable in interpreting the sequence of steps involved in the production of acrolein from propylene.

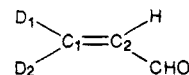
The data obtained by mass spectrometry has been interpreted on the basis of assuming that two products, $CD_2=CHCHO$ and $CH_2=CHCDO$, are formed during the oxidation of either $CD_3CH=CH_2$ or $CH_3CH=CD_2$.

The use of NMR provides the capability of accurately assigning the structure of the products.

The ¹H spectrum shown in Figure 7 exhibits only two signals, which can be assigned to the -CHO group of acrolein and the $CH_2=CH-$ group of acrolein. The presence of only two signals is consistent with the earlier proposal made on the basis of mass spectrometric data that only two isotopically labeled products are formed in the reaction.

The use of ²H and ¹³C NMR data, however, allows a rather detailed structural assignment of the products to be made. The proton broad band decoupled ²H NMR spectrum of the acrolein formed from the oxidation of $CH_3CH=CD_2$ is shown in Figure 8c. The spectrum suggests that the deuterium label is located at two different positions.

The chemical shifts were determined by using $CDCl_3$ as a reference (δ 7.24, see Figure 10). The signal at δ 9.57 can be assigned to the deuterium in $CH_2=CHCDO$. The two signals of equal intensity at δ 6.42 and 6.24 can be assigned to the deuterium in $CD_2=CHCHO$. The presence of these two signals of equal intensity indicate that the two deuterium atoms in $CD_2=CDCHO$ are magnetically nonequivalent, due to the presence of the C-2 asymmetric center.



The use of the double-labeled propylene, $^{13}CH_2=CHCD_3$, allows the chemical shifts of D_1 and D_2 to be determined. Oxidation of $^{13}CH_2=CHCD_3$ will lead to the formation of

(33) Isaev, O. V.; Margolis, L. Ya. *Kinet. Katal.* **1960**, *1*, 237.

(34) Trimm, D. L.; Gabbay, D. S. *Trans. Faraday Soc.* **1971**, *67*, 2782.

(35) Godin, G. W.; McCain, C. C.; Porter, E. A. *Proc. Int. Congr. Catal.* **1971**, *271*.

(36) Shchukin, V. P.; Borevskov, G. K.; Ven'yaminov, S. A.; Tarasova, D. V. *Kinet. Katal.* **1970**, *11*, 123.

(37) Allison, J. N.; Goodard, W. A., III In *Solid State Chemistry in Catalysis*; Grasselli, R. K., Brazdil, J. F., Eds.; American Chemical Society: Washington, D.C., 1985; p 24.

$^{13}\text{CH}_2=\text{CHCDO}$ and $\text{CD}_2=\text{CH}^{13}\text{CHO}$. Each of the two deuterium signals in $\text{CD}_2=\text{CH}^{13}\text{CHO}$ will be split into a doublet due to the vicinal coupling between D and ^{13}C . The coupling constants (J_{CD}) can be calculated from the results obtained for $^3J_{\text{CH}}$ by Vogeli et al.²⁷ from the following equation:

$$^3J_{\text{CD,calcd}} = \frac{^3J_{\text{CH}}}{\gamma_{\text{H}}/\gamma_{\text{D}}} \quad (3)$$

where γ_{H} and γ_{D} are the gyromagnetic ratios for a proton and a deuteron, respectively.

The experimental results presented in Table VI are in good agreement with those calculated from eq 3. The coupling constant for the trans deuterium is 2.4 Hz (2.5 from $^3J_{\text{CH}}$) and 1.6 Hz (1.6 from $^3J_{\text{CH}}$) for the deuterium cis to the carbonyl carbon. Using these coupling constants, it is possible to assign the chemical shift at 6.42 ppm to the deuterium trans to the carbonyl carbon (D_1) and the chemical shift at 6.24 ppm to the cis deuterium (D_2).

The small signal at δ 6.38, Figure 8c, can be assigned to acrolein with a deuterium at C-2 by comparing the results obtained for the oxidation of $\text{CH}_2=\text{CDCH}_3$ (Figure 11). Only one signal, corresponding to $\text{CH}_2=\text{CDCHO}$, is detected (δ 6.38). The DEPT ^{13}C spectrum (Figure 12) also indicates that a deuterium atom is located at C-2. This very minor product is produced by a mechanism not yet explained.

The ratio of the various forms of deuterated acrolein, $\text{CD}_2=\text{CHCHO}$ and $\text{CH}_2=\text{CHCDO}$, were calculated by comparing the amount of D_2 (preferred due to better resolution) or D_1 with that of $-\text{CDO}$. The data summarized in Table VII indicate that a 50:50 ratio was obtained for the oxidation of $\text{CD}_2=\text{CHCH}_3$, $\text{CH}_2=\text{CHCD}_3$, and $^{13}\text{CH}_2=\text{CHCD}_3$ over iron-antimony catalysts. This suggests that a common intermediate is formed from $\text{CD}_2=\text{CHCH}_3$ and $\text{CH}_2=\text{CHCD}_3$. As suggested earlier, this intermediate is a symmetrical π -allylic intermediate.

This 50:50 ratio also agrees with the results reported by Burdington et al.¹¹ They observed very nearly equal amounts of $\text{CD}_2=\text{CHCHO}$ and $\text{CH}_2=\text{CHCDO}$ produced during the oxidation of $\text{CH}_3\text{CH}=\text{CD}_2$ over antimony-based catalysts. They suggest that this ratio is a result of an irreversible addition of oxygen to the π -allyl intermediate to form the σ -allyl intermediate. This sequence provides a reasonable explanation for our suggestion that with antimony-based catalysts oxygen is added before the second hydrogen is abstracted.

Another possible explanation of the 50:50 ratio of the deuterated acrolein would be rapid double bond isomerization of propylene before the π -allylic intermediate is formed. This possibility can be ruled out, however, by examining the position of D (or ^{13}C) in the recovered unreacted propylene. The data in Table VII indicates that less than 8% of deuterium scrambling takes place before reaction. The ^{13}C data indicates that less than 2% double bond isomerization takes place. Thus, the evidence is quite conclusive that the 50:50 ratio cannot be explained by a rapid isomerization of propylene.

Conclusions

The selective oxidation of propylene over iron-antimony catalysts is kinetically and mechanistically very similar to the selective oxidation of propylene reported for $\text{USb}_3\text{O}_{10}$.¹³ The reaction proceeds via a redox mechanism and the selective lattice oxygen is confined to a thin surface layer, only several monolayers thick. The abstraction of an allylic hydrogen from propylene to form a π -allyl intermediate is the rate-limiting step and oxygen addition to form a σ -allyl intermediate occurs before the abstraction of a second hydrogen. Carbon dioxide is formed almost exclusively by the further oxidation of acrolein.

Registry No. Sb_2O_4 , 1332-81-6; FeSbO_4 , 15600-71-2; D_2 , 7782-39-0; propylene, 115-07-1.

Solid/Solid Interactions. Monolayer Formation in $\text{MoO}_3/\text{Al}_2\text{O}_3$ Physical Mixtures

J. Leyrer, M. I. Zaki,[†] and H. Knözinger*

Institut für Physikalische Chemie, Universität München, 8000 München 2, West Germany
(Received: January 30, 1986)

The so-called monolayer dispersion in physical mixtures of MoO_3 and $\gamma\text{-Al}_2\text{O}_3$ has been studied in the temperature range 723–823 K by laser Raman spectroscopy and low-temperature infrared spectroscopy of adsorbed carbon monoxide. It is shown that monolayer dispersion or spreading only occurs in the presence of water vapor, which volatilizes MoO_3 with formation of $\text{MoO}_2(\text{OH})_2$. The dispersion mechanism in this system is considered as surface diffusion of $\text{MoO}_2(\text{OH})_2$ in a concentration gradient with additional contributions from gas-phase transport. An explanation of the dispersion phenomenon as wetting of one solid by another solid under the action of the surface tension is considered less likely.

Introduction

Molybdate catalysts supported on alumina represent one of the technologically most important class of solid catalysts. They are usually prepared by impregnation of the alumina support from aqueous solution of ammonium heptamolybdate. It is well-known today^{1,2} that the molybdenum species in these catalysts in their oxide precursor state can be described as surface analogues of molybdenum polyanions.

Xie and co-workers first showed³ that heating a physical mixture of crystalline MoO_3 and $\gamma\text{-Al}_2\text{O}_3$ at temperatures near 670 K for typically 24 h led to the disappearance of the X-ray diffraction pattern of MoO_3 . This observation was interpreted as monolayer dispersion of MoO_3 on the surface of $\gamma\text{-Al}_2\text{O}_3$, and a monolayer

capacity of 0.12 g of $\text{MoO}_3/100 \text{ m}^2$ was estimated. In a series of subsequent papers, the same group reported supportive data for the same oxide combination⁴⁻⁸ and for crystalline MoO_3

(1) Jeziorowski, H.; Knözinger, H. *J. Phys. Chem.* **1979**, *83*, 1166.

(2) Leyrer, J.; Vielhaber, B.; Zaki, M. I.; Zhuang, Shuxian; Weitkamp, J.; Knözinger, H. *Mater. Chem. Phys.* **1985**, *13*, 301.

(3) Liu, Yingjun; Xie, Youchang; Ming, Jing; Liu, Jun; Tang, Youqi *Cuihua Xuebao* **1982**, *3*, 262.

(4) Liu, Ying-Jun; Xie, Youchang; Li, Ce; Zou, Zhi-yang; Tang, Youqi *Cuihua Xuebao* **1984**, *5*, 234.

(5) Xie, Youchang; Gui, Linlin; Liu, Yingjun; Zhao, Biying; Yang, Naifang; Zhang, Yufen; Guo, Quinlin; Duan, Lianyun; Huang, Huizhong; Cai, Xiaohai; Tang, Youchi *Proc. Int. Congr. Catal.*, *8th*, **1984**, *5*, 147.

(6) Xie, Youchang; Gui, Linlin; Liu, Yingjun; Zhang, Yufen; Zha, Biying; Yang, Naifang; Guo, Quinlin; Duan, Lianyun; Huang, Huizhong; Cai, Xiaohai; Tang, Youchi *In Adsorption and Catalysis on Oxide Surfaces*; Che, M., Bond, G. C., Eds.; Elsevier: Amsterdam, 1985; p 139.

[†] Permanent address: Chemistry Department, Faculty of Science, Minia University, El-Minia, Egypt.